Available online at www.sciencedirect.com
SCIENCE DIRECT®
Journal of Solid State Chemistry 177 (2004) 3675–3681
JOURNAL OF SOLID STATE CHEMISTRY
http://elsevier.com/locate/jssc

A new technique for preparing macroporous inorganic composite material

Yan-Bo Zhang, Hua-Feng Shao, Xue-Feng Qian,* Jie Yin, and Zi-Kang Zhu

State Key Laboratory of Composite Materials, School of Chemistry and Chemical Technology, Research Institute of Polymer Materials, Shanghai Jiao Tong University, Shanghai 200240, PR China

Received 28 April 2004; received in revised form 10 June 2004; accepted 10 June 2004

Available online 3 September 2004

Abstract

Macroporous CdS/SiO_2 was prepared with a new approach in which at first CdS nanoparticles were deposited on polymer microbeads without surfactant, then core-shell composite was self-assembled with sedimentation-aggregation, and at last macroporous material was obtained by the removal of the template. The results show that the morphology of core-shell composite could be tailored by the polymer template and the concentration of the reactant, and the shell thickness could be altered by the temperature and the aging time. This new idea was an effective method to prepare other macroporous composite with large-scale.

Keywords: Self-assembly; Macroporous; Composite; Cadmium sulfide; Silica

1. Introduction

In the last few years, macroporous materials have attracted much attention because of their current and future potential applications in various fields, such as optical information processing and storage [1], photonic band gap materials [2] due to its pore size dependence. Furthermore, nano-size effects can be produced if the skeletal dimensions can be small enough [3]. The range of macroporous materials prepared includes metals [4], metal oxides [5], polymers [6], and carbon [7], etc. Among them, macroporous semiconductors attracted more attention because they possess the characters of high refractive index, efficient luminescence and optical nonlinearities on which many applications of photonic crystals rely [8].

To synthesis those macroporous structural materials, physical, chemical and engineering methods have been applied which included sol–gel technique [9], salt precipitation [10] and particle infusion [11], etc. Among them, one novel route is that macroporous materials were obtained from the coated spheres. For example, Caruso et al. [12] synthesized macroporous inorganic composite material in which firstly PS/silica core-shell spheres assembled by infiltration of titanium precursor into them, then macroporous composite material was obtained by removal of the spheres.

The method could fabricate macroporous materials with controlled pore morphologies because the pore wall thickness and the pore strucutures could be tailored by the thickness or concentration of shell in the core-shell spheres. And tailored pore morphologies could lead to different properties of macroporous materials, such as density, thermal conductivity and pore volume [13].

Here we report a new technique for preparing macroporous CdS/SiO_2 with long-range micrometer scale. Compared with previous methods mentioned above, PS spheres were coated with tailored CdS shell without any surfactant, then assembly of core-shell composite was prepared with the sol–gel technique and sedimentation aggregation, and at last, macroporous material was obtained with removal of polymer spheres.

2. Experimental

2.1. Materials

Styrene (AR, Shanghai Lingfeng Chemical Reagent Co., Ltd.) was purified by reduced pressure distillation.

*Corresponding author. Fax: +86-21-5474-1297.
E-mail address: xfqian@mail.sjtu.edu.cn (X.-F. Qian).

0022-4596/$ - see front matter © 2004 Elsevier Inc. All rights reserved.
doi:10.1016/j.jssc.2004.06.022

Dodecyl sodium sulfate (AR, Shanghai Lingfeng Chemical Reagent Co., Ltd.) and potassium persulfate (AR, Shanghai Qianjin reagent factory) were recrystallized twice in water. Cadmium acetate ($Cd(Ac)_2 \cdot 2H_2O$), thioacetamide (TAA), polyvinyl pyrrolidone (PVP) and tetraethoxysilane (TEOS, 28%) were all purchased from Shanghai Reagent Company and used without further purification.

2.2. Polystyrene microbeads

Non-cross linked, monodispersed PS particles were synthesized by emulsifier-free emulsion polymerization [14].

2.3. Core-shell composite

In a typical process to fabricate the PS/CdS core-shell composite, 50 mg PS beads, 436.3 mg $Cd(Ac)_2 \cdot 2H_2O$, 123 mg TAA and 50 g H_2O were added to the conical flask. The mixture was aged for 4 h at 80°C. Then the mixture was centrifugated and washed with ethanol and water several times. After being dried in the vacuum oven, the core-shell samples were obtained.

2.4. Hollow CdS spheres and macroporous CdS

In a typical process to self-assemble PS/CdS core-shell composite, 0.05 g of composite was added to 1.0 g of absolute ethanol and 7×10^{-5} mol of TEOS was added to the above solution. Then, the solution was stirred for about 20 min and aged at the ambient temperature for about 24 h. After being dried in the vacuum oven, the as-synthesized samples were obtained.

To prepare CdS hollow spheres or macroporous CdS, the as-synthesized PS/CdS core-shell particles or their assembly were dispersed in the toluene for 24 h, then centrifugated and washed with toluene several times and redispersed in toluene. The process was repeated several times to remove the PS core. The sample was dried in the vacuum oven before characterization.

2.5. Characterization

Hitachi H-8100 transmission electron microscope (TEM) and JEOL JSM-6360LV scanning electron microscopy (SEM) were employed to obtain TEM and SEM images, respectively. The powder X-ray diffraction (XRD) patterns were recorded on a Bruker-AXS D8 ADVANCE X-ray diffractometer at a scanning rate of 4°/min in 2θ ranging from 10° to 70° with Cu$K\alpha$ radiation ($\lambda = 0.1542$ nm). Ultraviolet–visible (UV–Vis) spectra were measured on a Perkin–Elmer Lambda 20 UV–Vis transmission spectrophotometer, and spectrum from suspension was obtained from sample contained in quartz cells. IR spectra were recorded on a Perkin–Elmer Paragon 1000 spectrometer. The samples were grounded with KBr cystal and the mixture of them was pressed into a flake for IR measurement. The thermogravimetric analysis (TGA) was operated on a Perkin–Elmer TGA 7 analyzer at a heating rate of 20°C/min under the stream of nitrogen.

3. Results and discussion

3.1. Preparation of PS/CdS core-shell composite and its hollow spheres

Table 1 lists the condition of the preparation of core-shell composite and their morphologies. PS and CdS spheres are named as samples 1 and 2, respectively.

Fig. 1(a) is the TEM image of polystyrene microbeads (sample 1 in Table 1) and (b) CdS particles (sample 2), which are both monodispersed with the diameter of ~300 and 500 nm, respectively.

Sample 3 was prepared by aging the solution of PS, $Cd(Ac)_2$, TAA, and PVP, and the TEM image is shown in Fig. 2(a). It can be seen that rough-coated CdS/PS microspheres were obtained. CdS particles deposited on the surface of PS were less than 500 nm in diameter because the deposition of CdS nanoparticles was through heterocoagulation process, in which the

Table 1
Properties of PS/CdS core-shell microspheres obtained from different conditions

Sample	PS (g/dm^{-3})	$Cd(Ac)_2$ (mol/dm^{-3})	TAA (mol/dm^{-3})	PVP (g/dm^{-3})	Time (h)	Temperature (°C)	Particle diameter (nm)	System characteristics[a]
1	0.001	—	—	—	—	—	300	Monodispersity
2	—	3.27	3.27	0.02	2	80	500	Monodispersity
3	0.001	3.27	3.27	0.02	2	80	~350	R, M
4	0.001	3.27	3.27	—	2	80	~350	S
5	0.001	3.27	9.81	—	2	80	~350	S, M
6	0.001	9.81	3.27	—	2	80	~350	R, M
7	0.001	3.27	3.27	—	4	25	~380	S
8	0.001	3.27	3.27	—	1	120	~370	S, M

[a] S: smooth coated spheres; R: rough-coated spheres; M: mixed systems containing coated spheres and separated CdS particles.

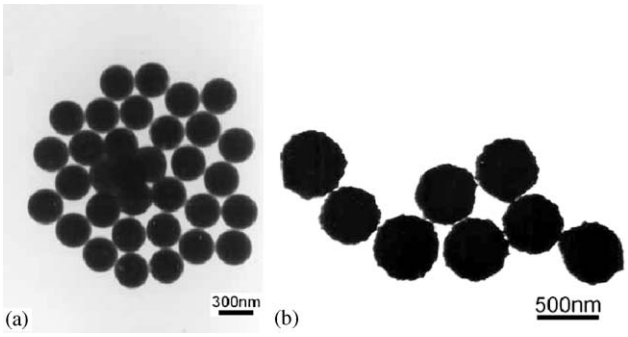

Fig. 1. TEM images of (a) sample 1, and (b) sample 2.

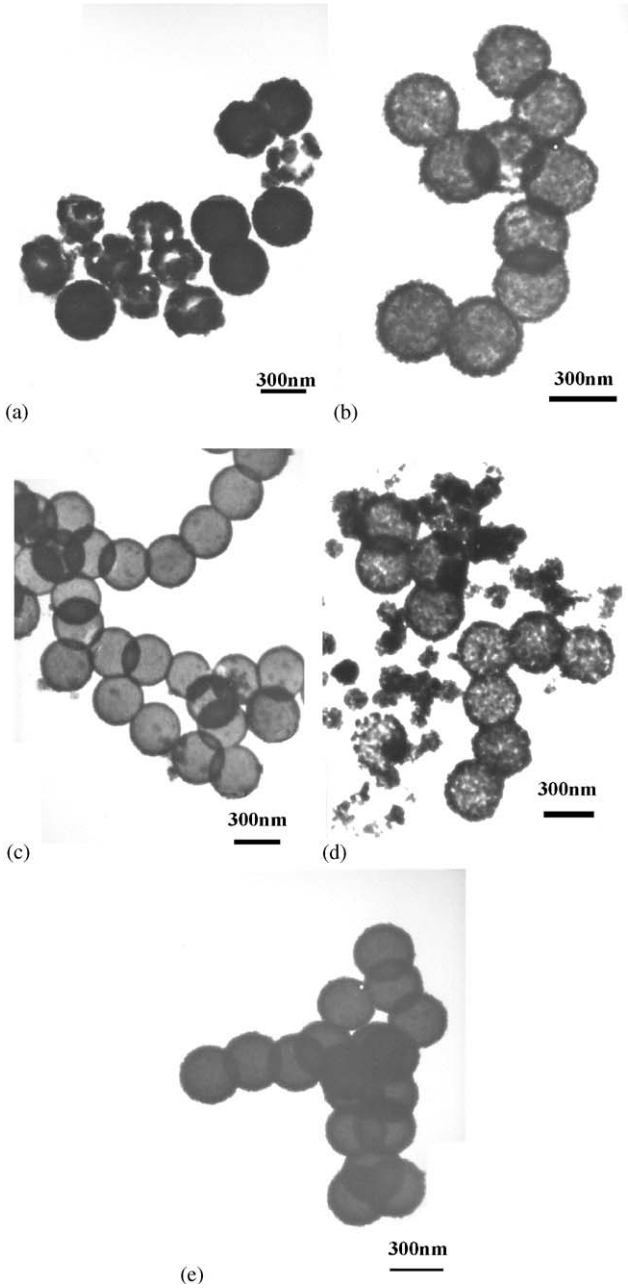

Fig. 2. TEM images of (a) sample 3, (b) sample 4, (c) sample 5, (d) sample 6, and (e) sample 7 according to Table 1.

formation of CdS nanoparticles and the deposition of CdS on PS surface happened simultaneously [15–18]. Compared to sample 3, smooth coated microspheres (samples 4–7) were also prepared in the aqueous solution of PS, TAA and Cd^{2+} without the presence of PVP. Without PVP, the aggregation of PS microbeads is also avoided due to the polarity of acetic acid which formed through the reaction of TAA and water. This can be found from the experiment. When PS particles were added into the solution of TAA, homogeneous latex emulsion solution was obtained, however, PS beads suspended on the surface of aqueous solution and were difficult to disperse in water without TAA. Fig. 2(b) shows the TEM image of sample 4, from which it can be found that the surface of the PS beads is coated with the CdS nanoparticles and the thickness of the shell is about 25 nm. Just as said above, the formation of PS core/CdS shell composite was through heterocoagulation of CdS on the surface of PS after S^{2-} reacted with Cd^{2+} during the decomposition of TAA.

The concentration of precursors has much influence on the morphologies of the core-shell microspheres. Samples 5 and 6 (TEM images shown in Figs. 2(c) and (d), respectively) in Table 1 were obtained with high concentration of TAA and $Cd(Ac)_2$, respectively. It can be seen that sample 5 contains coated spheres and separated small CdS particles. With the increase of $Cd(Ac)_2$ concentration, more separated greater CdS particles formed in sample 6 (see Fig. 2(d)). Furthermore, the surface of sample 5 is smooth, while that of sample 6 is relatively rough. This indicates that the deposition of CdS nanoparticles on the surface of PS beads depended strongly on the concentration of the precursors.

The effect of temperature on the surface morphology and the formation of the composite particles are similar to the concentration. When sample 7 was prepared at room temperature, the surface of the sample is smoother than that of the sample prepared at a higher temperature. The surface of the sample prepared at a higher temperature is also smooth, but some of isolated CdS particles could be found. The reason is that at a higher temperature, the formation of CdS is faster than the hetero-deposition of CdS particles on the template. The aggregation of CdS leads to the formation of large CdS particles, and their subsequent deposition on the surface of PS beads results in the formation of rough-coated surface. The most compact and smooth surface of the sample is obtained at room temperature and its shell thickness is about 40 nm from Fig. 2(e) and there are no isolated CdS nanoparticles in the system. Sample 8 is obtained at 120°C (TEM image is not shown here), and the existence of the isolated CdS nanoparticles is also the evidence of the effect of high temperature on the deposition.

CdS hollow spheres can be obtained through the dissolution of PS core with organic solvents such as

toluene. Fig. 3 is the TEM image of CdS hollow spheres obtained from sample 7. From the photograph, it could be found that most of micropheres were intact indicating that removal PS spheres by dissolution with organic solution is an effective method to obtain hollow spheres or macroporous material with stable structure. Some were broken during the dissolution probably because of the enlargement of the volume of PS core due to swelling.

In order to further confirm whether PS cores were removed completely through dissolution or not, the TGA analysis was adopted. PS microspheres completely decomposed before 450°C from Fig. 4(a). The first weight loss stage of sample 7 (Fig. 4(b)) and hollow spheres (Fig. 4(c)) is the release of water between 50°C and 200°C. The second weight loss stage of curve b, between 350°C and 450°C, corresponds to the weight loss of PS, and the remaining weight is 82% which is consistent with the weight percentage of PS in the core-shell composite. Curve c shows no obvious weight loss at 350–450°C, indicating that the PS template can be completely removed through dissolution.

IR spectra and XRD patterns were also used to confirm the formation of PS/CdS core-shell and CdS hollow structures.

The possible mechanism for the formation PS/CdS core-shell composites is illustrated in Scheme 1. From the discussions above, the increase in the concentration of $Cd(Ac)_2$ favors the formation of larger CdS crystallites and rough-coated composite particles. This is illustrated in the path 2 of Scheme 1 which is corresponding to sample 6 and Fig. 2(d). The increase

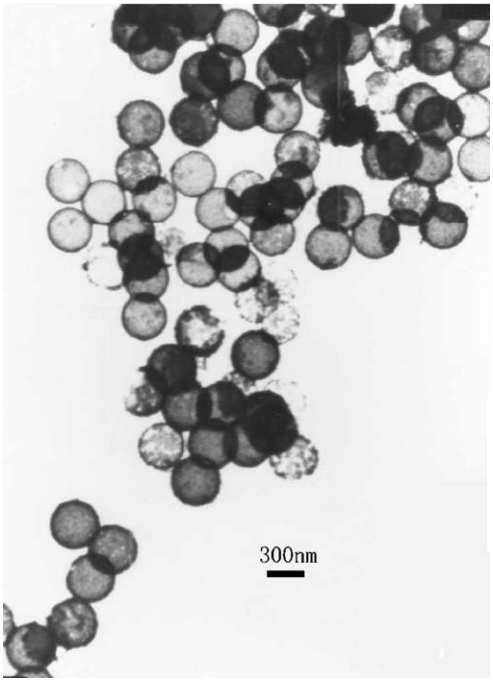

Fig. 3. TEM images of hollow spheres of sample 7.

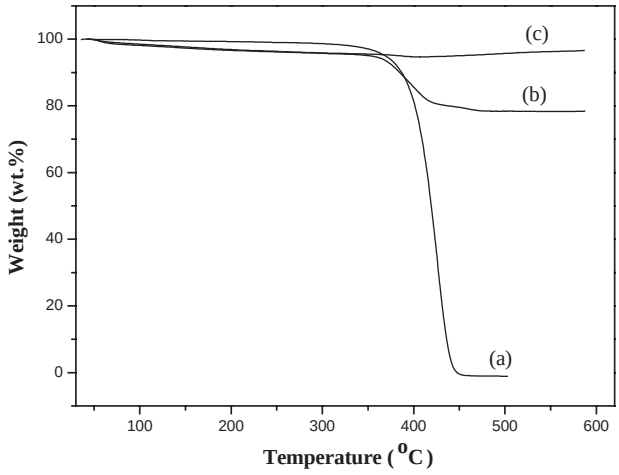

Fig. 4. Thermo gravimetric traces of (a) sample 1 (PS), (b) sample 7 (PS/CdS), and (c) hollow spheres of CdS obtained from sample 7.

in the concentration of TAA favors the formation of relatively smaller CdS crystallites and smooth-coated spheres. This is illustrated in path 3 of Scheme 1 which is corresponding to sample 5 and Fig. 2(c). The reason is due to that when the concentration of TAA is high, the rapid decomposition of TAA leads to a rapid release of S^{2-} ions. Subsequently, a great number of smaller crystalline CdS forms as precipitation center or deposits on another crystalline center, then fine particles form and deposit on the surface of PS beads leading to the formation of smooth surface spheres. Some fine particles are too late to deposit and are present as isolated particles [19,20]. When the concentration of Cd^{2+} ion is high, the in situ formation rate of small CdS nanoparticles increases, resulting in the aggregation or the formation of large CdS particles as well as high deposition rate on the PS surface [21,22]. When the molar ratio of $[Cd^{2+}]/[S^{2-}]$ is about 1, the smoothest surface coated core-shell composites form. This process is illustrated in path 1 of Scheme 1 which is corresponding to sample 7 and Fig. 2(e). It is also the result of controlling the sulfide ion release rate which depends on the concentration of TAA in the solution.

3.2. Preparation of macroporous CdS composite and its property

Fig. 5 shows the SEM image of PS/CdS core-shell composites, from which it can be found that PS beads were completely and compactly coated with nano-sized CdS particles. The detailed process for preparing macroporous CdS composite was shown in Scheme 2. At first, PS/CdS core-shell composites were obtained which are discussed above. Then large-scale arrays of PS/CdS core-shell composites were obtained after those composites were self-assembled through the sol–gel process with the help of TEOS. At last, large-scale

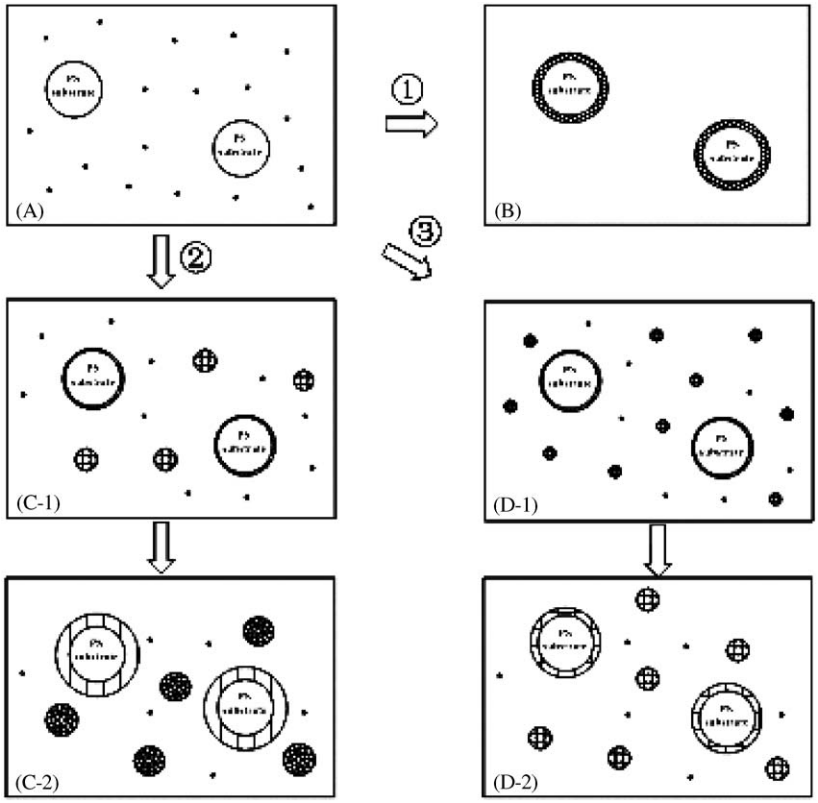

Scheme 1. Schematic description of the mechanism of core-shell composites formation.

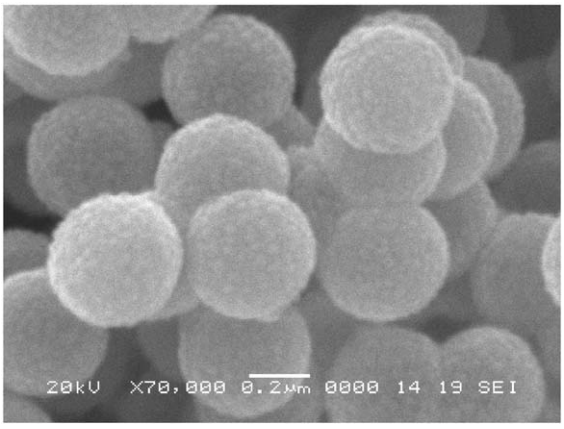

Fig. 5. SEM images showing sample 7.

macroporous CdS/SiO_2 material was obtained after the obtained large-scale arrays were dissolved to remove PS cores. Figs. 6(a) and (b) show close and general views of macroporous composite, respectively. It indicates that large-scale macroporous CdS composite could be obtained successfully and the connected pores could be obtained with the network of CdS and –Si–O– conducted by the hydrolysis of silica source [23]. From Fig. 6(a), PS cores are completely removed. From Fig. 6(b), the solid of macroporous CdS/SiO_2 is at least hundreds of micron in length and width. In the preparation process of macroporous CdS, the concentration of TEOS in the composition of precursors is the key factor and has great effects on the morphology of the final product. When the concentration of TEOS is below 0.07 mmol/g ethanol, assembly of PS/CdS was obtained, while only single $PS/CdS/SiO_2$ core-shell microbeads were obtained when the concentration of TEOS in the solution is more than 0.1 mmol/g ethanol. When the TEOS concentration is high, during the process of stirring, the sol–gel reaction of TEOS is fast enough to obtain the samples with the structure of PS and CdS core-SiO_2 shell in the process of sol–gel and before the process of sedimentation. On the other hand, when the concentration of TEOS is down to 0.05 mmol/g ethanol, the percentage of macroporous CdS solid is low because a lot of PS core/CdS shell spheres could not be assembled with hydrolyzation of TEOS. So the array process of core-shell composite includes the sel–gel technique of TEOS which links the PS/CdS spheres and the process of sedimentation-aggregation, and the two processes are so interdependent that the final macroporous structured sample will not be obtained if the two processes are not going along simultaneously.

Fig. 7 shows the X-ray diffraction patterns (XRD) of macroporous CdS/SiO_2 composite. The pattern shows that the sample is cubic structure CdS nanocrystals. Three main peaks can be indexed as (111), (220) and (311) of CdS crystals. The broadening of the peak

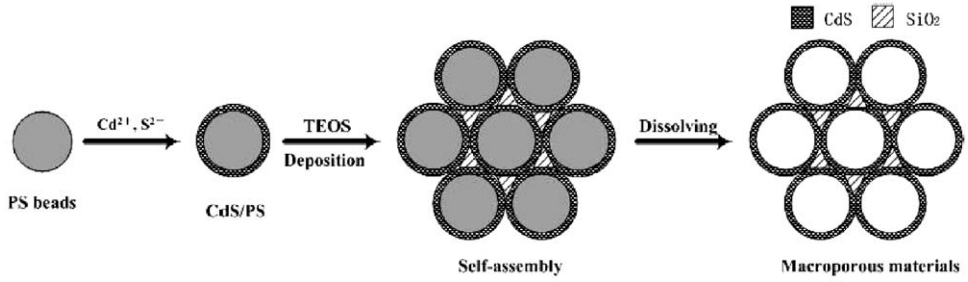

Scheme 2. Schematic description of preparation process of macroporous sample.

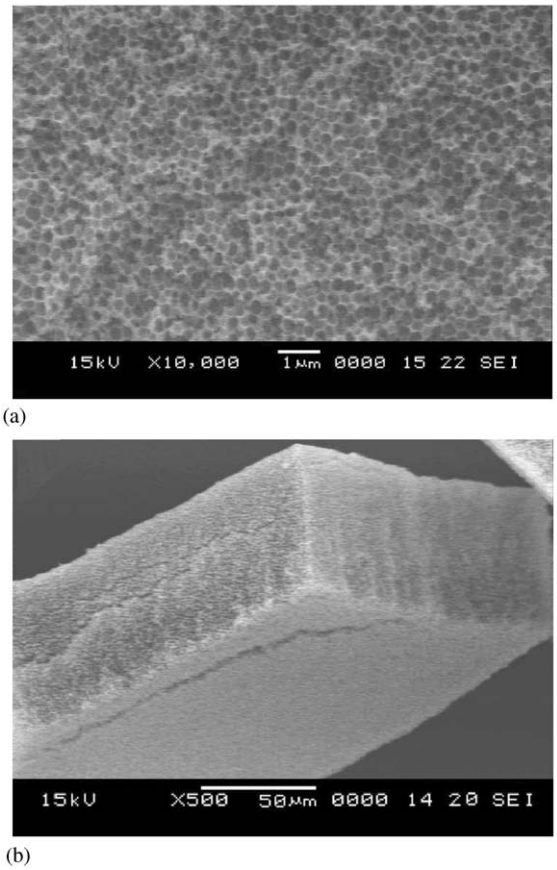

Fig. 6. SEM images showing (a) close view, and (b) general view of macroporous sample.

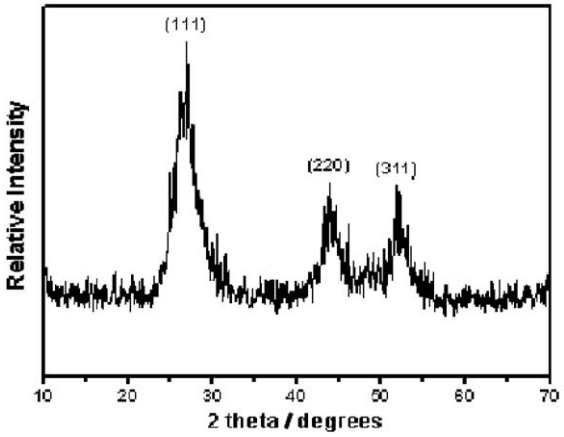

Fig. 7. XRD pattern of macrostructured samples.

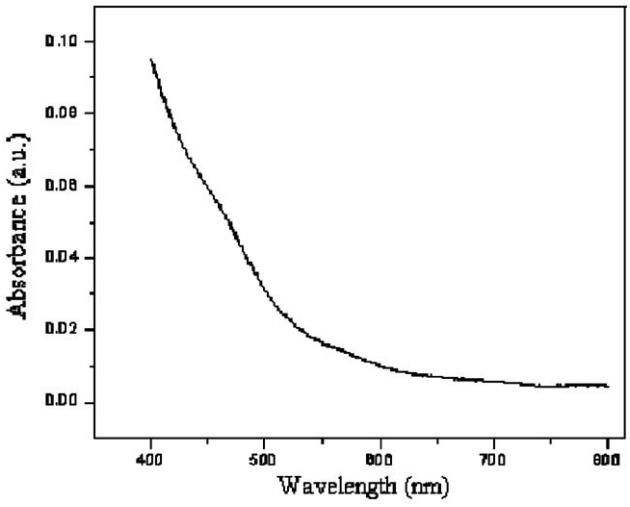

Fig. 8. UV–Vis absorption spectrum of macroporous material.

indicates that the walls of macroporous CdS are constructed with much smaller CdS nanoparticles. The XRD pattern does not show the peaks of silica due to its amorphous structure.

Fig. 8 is the UV–Vis absorption spectrum of macroporous material which shows an absorption onset at about 470 nm, being blue-shifted compared to bulk CdS (512 nm). This blue shift was caused by strong quantum confinement effect, due to the decrease in particle size [24]. Calculations of the average particle size were made employing the Brus formula [25] and estimations based on this absorption value suggested the presence of particles with an average diameter of about 7 nm. To determine the band gap, we fit the absorption data to Eq. (1) by extrapolating the linear portions of the curves to absorption equal to zero [26]:

$$\alpha h\nu = A(h\nu - E_g)^{1/2}, \quad (1)$$

where α is the absorption coefficient, $h\nu$ the photo energy, E_g the direct band gap, and A a constant. The

band gap of material was calculated to be about 2.80 eV, larger than that of the bulk materials (2.5 eV).

Thermal property of macroporous composite material was carried out with muffle furnace and the morphology characteristics of the sample were measured by means of SEM. At 550°C, the macroporous structure begins to deteriorate at the wall between the connected pores, but a large part of the macroporous structure is still intact. At higher temperature, such as 700°C, a severe collapse of the macroporous structure occurs, leading to the formation of larger defects and ultimately to the particles.

4. Conclusions

In this paper, macroporous CdS/SiO_2 was successfully prepared in large scale with the techniques combining sol–gel and sedimentation aggregation processes. Firstly PS core-CdS shell composite was obtained by the heterogeneous deposition of nanoparticles on PS beads. Then sol–gel and sedimentation aggregation techniques were used to synthesize the assembly of core-shell composite. Finally macroporous CdS was achieved through dissolving PS cores. The results show that it is important to control the processes of the sol–gel and sedimentation aggregation. Although the array of macropores is not more regular than that of samples prepared from the pre-prepared ordered colloidal template, macroporous structured materials could be obtained in large-scale through this method. The approach could produce macroporous semiconductor in macroscopic scale and prepare other II–VI and III–V semiconductors or semiconductors.

Acknowledgments

This work was financially supported by the National Natural Foundation of China (50103006), the Shanghai Shu Guang Project and the Shanghai Nanomaterials Project (0241nm106).

References

[1] D.O. Velev, E.W. Kaler, Adv. Mater. 12 (2000) 7.
[2] G.R. Yi, J.H. Moon, S.M. Yang, Chem. Mater. 13 (2001) 2613–2618.
[3] A. Stein, R.C. Schroden, Curr. Opin. Solid State Mater. Sci. 5 (2001) 553–564.
[4] J.E.G.J. Wijnhoven, S.J.M. Zenvenhuizen, M.A. Hendriks, D. Vanmaekelbergh, J.J. Kelly, W.L. Vos, Adv. Mater. 12 (2000) 888–890.
[5] C.F. Blanford, H. Yan, R.C. Schroden, M. Al-Daous, A. Stein, Adv. Mater. 12 (2001) 401–407.
[6] P. Jiang, K.S. Hwang, D.M. Mittleman, J.F. Bertone, V.L. Clovin, J. Am. Chem. Soc. 121 (1999) 11630–11637.
[7] A.A. Zakhidov, R.H. Baughman, Z. Iqbal, C.X. Cui, I. Khayrullin, S.O. Dantas, I. Marti, V.G. Ralchenko, Science 282 (1998) 897.
[8] Y.A. Vlasov, N. Yao, D.J. Norris, Adv. Mater. 11 (1999) 2.
[9] A. Imhof, D.J. Pine, Nature 389 (1997) 948.
[10] H.W. Yan, C.F. Blanford, B.T. Holland, M. Parent, W.H. Smyrl, A. Stein, Adv. Mater. 11 (1999) 1003.
[11] O.D. Velev, P.M. Tessier, A.M. Lenhoff, E.W. Kaler, Nature 401 (1999) 548.
[12] D. Wang, R.A. Caruso, F. Caruso, Chem. Mater. 13 (2001) 364–371.
[13] (a) J.E.G.J. Wijnhoven, W.L. Vos, Science 281 (1998) 802;
(b) B.T. Holland, C.F. Blanford, A. Stein, Science 281 (1998) 538;
(c) M. Wu, T. Fujiu, G.L. Messing, J. Non-Cryst. Solids 121 (1990) 407.
[14] J.H. Kim, M. Chainey, M.S. El-Aasser, J.W. Vanderhoff, J. Polym. Sci. A: Polym. Chem. 27 (1989) 3187.
[15] N. Kawahashi, H. Shiho, J. Mater. Chem. 10 (2000) 2294.
[16] N. Kawahashi, C. Persson, E. Matihevic, J. Mater. Chem. 1 (1991) 577.
[17] H. Shiho, N. Kawahashi, J. Colloid Interface Sci. 226 (2000) 91.
[18] H. Shiho, Y. Manabeb, N. Kawahashia, J. Mater. Chem. 10 (2000) 333.
[19] S. Libert, D.V. Goia, E. Matijevic, Langmuir 19 (2003) 10673–10678.
[20] S. Libert, V. Gorshkov, D. Goia, E. Matijevic, V. Privman, Langmuir 19 (2003) 10679–10683.
[21] K. Yamaguchi, T. Yoshida, T. Sugiura, H. Minoura, J. Phys. Chem. B 102 (1998) 9677.
[22] K. Yamaguchi, T. Yoshida, D. Lincot, H. Minoura, J. Phys. Chem. B 107 (2003) 387.
[23] T. Torimoto, J.P. Reyes, S. Murakami, B. Pal, B. Ohtani, J. Photochem. Photobiol. A: Chemistry 160 (2003) 69–76.
[24] L.E. Brus, J. Chem. Phys. 80 (1984) 4403.
[25] L.E. Brus, J. Chem. Phys. 79 (1983) 5566.
[26] Y. Wang, A. Sunna, W. Mahler, R. Kasowski, J. Chem. Phys. 87 (1987) 7315.